Spermine and spermidine bind CXCR4 and inhibit CXCR4- but not CCR5-tropic HIV-1 infection

Mirja Harms, Nikaïa Smith, Mingyu Han, Rüdiger Groß, Pascal von Maltitz, Christina Stürzel, Yasser Ruiz-Blanco, Yasser Almeida-Hernández, Armando Rodriguez-Alfonso, Dominique Cathelin, et al.

VIROLOGY

Spermine and spermidine bind CXCR4 and inhibit CXCR4- but not CCR5-tropic HIV-1 infection

Mirja Harms[1]†, Nikaïa Smith[1,2,3]†, Mingyu Han[3], Rüdiger Groß[1], Pascal von Maltitz[1], Christina Stürzel[1], Yasser B. Ruiz-Blanco[4], Yasser Almeida-Hernández[5], Armando Rodriguez-Alfonso[6,7], Dominique Cathelin[2,8], Birgit Caspar[2,8], Bouceba Tahar[9], Sophie Sayettat[3], Nassima Bekaddour[2,8], Kanika Vanshylla[10], Franziska Kleipass[10], Sebastian Wiese[7], Ludger Ständker[6], Florian Klein[10,11,12], Bernard Lagane[13], Arnaud Boonen[14], Dominique Schols[14], Serge Benichou[3], Elsa Sanchez-Garcia[4,5], Jean-Philippe Herbeuval[2,8]*, Jan Münch[1]*

Semen is an important vector for sexual HIV-1 transmission. Although CXCR4-tropic (X4) HIV-1 may be present in semen, almost exclusively CCR5-tropic (R5) HIV-1 causes systemic infection after sexual intercourse. To identify factors that may limit sexual X4-HIV-1 transmission, we generated a seminal fluid–derived compound library and screened it for antiviral agents. We identified four adjacent fractions that blocked X4-HIV-1 but not R5-HIV-1 and found that they all contained spermine and spermidine, abundant polyamines in semen. We showed that spermine, which is present in semen at concentrations up to 14 mM, binds CXCR4 and selectively inhibits cell-free and cell-associated X4-HIV-1 infection of cell lines and primary target cells at micromolar concentrations. Our findings suggest that seminal spermine restricts sexual X4-HIV-1 transmission.

INTRODUCTION

Entry of the human immunodeficiency virus (HIV-1) into target cells is mediated by binding of the viral envelope glycoprotein gp120 to the CD4 receptor and a subsequent interaction with one of the two major co-receptors, CCR5 or CXCR4 (*1*). HIV-1 variants using CCR5 (R5-HIV-1) predominate, while CXCR4-tropic HIV-1 (X4-HIV-1) only occurs in approximately 50% of nontreated patients, and are associated with a more rapid deterioration of the immune system (*2*–*5*). Blockade of CXCR4 or CCR5 with chemokines, antibodies, or small molecules can prevent HIV-1 infection, and CCR5 inhibitors such as maraviroc have been approved as therapeutics (*6*, *7*).

Most HIV-1 transmission events are a result of unprotected sexual intercourse, and semen is considered an important vector for viral dissemination (*8*). Upon deposition of virus-contaminated semen in the recipient's anogenital tract, HIV-1 crosses the mucosal epithelial barrier most likely via small tissue microlesions to reach susceptible target cells, thereby establishing a small founder population of infected cells. After local expansion, infected cells and virus disseminate toward draining lymph nodes and subsequently establish a systemic self-propagating infection (*9*). In most of the cases, primary infection is established by a single virion, termed the transmitted/founder (T/F) virus (*10*–*12*). Transmission of individual HIV-1 variants is not a random event, and T/F HIV-1 assembles specific characteristics (*13*–*17*). T/F viruses are almost exclusively R5-tropic, which can be expected because R5 viruses predominate in sexually active asymptomatic individuals. However, several studies demonstrated that even if X4 viruses are present in semen of the donor, only R5 or dual-tropic viruses finally establish a productive infection, with very few exceptions (*10*, *14*, *15*, *18*). Studies on the viral composition of the donor's semen and the recipient's mucosal tissue at the first time points after infection are very rare, and early infection events are extremely difficult to analyze. Still, these findings suggest the existence of a gate-keeping mechanism that prevents X4-HIV-1 transmission from infected males to their sex partners (*19*–*21*). The reasons for this bottleneck are largely unknown, and attempted explanations have lacked evidence (*20*, *22*). It has been proposed that X4-HIV-1 might be restricted at the level of adaptive immunity, as several reports observed a selective repression of X4-HIV-1 at the time of antibody seroconversion (*23*–*26*). In addition, enriched expression of CCR5 in anogenital mucosa may facilitate R5-HIV-1 transmission (*27*–*30*), but cervical and rectal lymphocytes were shown to additionally express CXCR4, and both tissues can be infected by both R5-HIV-1 and X4-HIV-1 ex vivo and in humanized mouse models (*20*, *28*, *31*, *32*). Several groups also proposed an advantage of R5-HIV-1 over X4 virus variants on the level of either Langerhans cell (LC) infection or cell-to-cell transmission through the virological synapse (*33*–*37*). However,

[1]Institute of Molecular Virology, Ulm University Medical Center, 89081 Ulm, Germany. [2]CNRS UMR-8601, Université Paris Cité, 75006 Paris, France. [3]Institut Cochin, Inserm U1016, CNRS UMR8104, Université Paris-Cité, 75014 Paris, France. [4]Computational Biochemistry, Center of Medical Biotechnology, University of Duisburg-Essen, Universitätsstr. 2, 45141 Essen, Germany. [5]Computational Bioengineering, Department of Biochemical and Chemical Engineering, Emil-Figge Str. 66., 44227 Dortmund, Germany. [6]Core Facility Functional Peptidomics, Ulm University Medical Center, 89081 Ulm, Germany. [7]Core Unit Mass Spectrometry and Proteomics, Ulm University, 89081 Ulm, Germany. [8]Chemistry and Biology, Modeling and Immunology for Therapy (CBMIT), Paris, France. [9]Sorbonne University, CNRS, Institut de Biologie Paris-Seine (IBPS), Protein Engineering Platform, Molecular Interaction Service, F-75252 Paris, France. [10]Laboratory of Experimental Immunology, Institute of Virology, Faculty of Medicine and University Hospital Cologne, University of Cologne, 50931 Cologne, Germany. [11]German Center for Infection Research (DZIF), Partner site Bonn-Cologne, 50937 Cologne, Germany. [12]Center for Molecular Medicine Cologne (CMMC), University of Cologne, 50931 Cologne, Germany. [13]Infinity, Université de Toulouse, CNRS, INSERM, Toulouse, France. [14]Laboratory of Virology and Chemotherapy, Department of Microbiology, Immunology and Transplantation, Rega Institute, KU Leuven, Herestraat 49, P.O. Box 1030, 3000 Leuven, Belgium.
*Corresponding author. Email: jan.muench@uni-ulm.de (J.M.); jean-philippe.herbeuval@parisdescartes.fr (J.-P.H.)
†These authors contributed equally to this work.

those findings are controversial, and an involvement of LCs for HIV-1 infection under in vivo conditions is still under debate (*35*, *38*).

RESULTS

Spermine and spermidine in seminal plasma inhibit X4-tropic HIV-1

We here hypothesized that factors present in semen may specifically restrict X4-HIV-1 but not R5-HIV-1 infection. To identify these factors, molecules below 30 kDa were separated by reversed-phase high-performance liquid chromatography (RP-HPLC) (fig. S1A) from 2 ml of seminal plasma (SP), and the resulting 50 fractions were screened for inhibitory activity against X4-HIV-1 and R5-HIV-1 in TZM-bl reporter cells. As shown in Fig. 1A, fractions 15 to 18 resulted in a more than 90% reduced infection of X4-HIV-1 but not R5-HIV-1. As the RP-HPLC chromatogram at 280 nm indicated a low protein/peptide content of these fractions (fig. S1A), fraction 15 was subjected to mass spectrometric analysis. This showed the predominant presence of spermine and spermidine (fig. S1, B and C), two polyamines abundantly present in semen at concentrations of up to 14 and 0.6 mM, respectively (*39*). Thin-layer chromatography (TLC) of samples derivatized with dansyl chloride (fig. S2, A to C) confirmed the presence of spermine, and to a lesser extent spermidine, in the X4-HIV-1 inhibitory fractions 15 to 18, while both polyamines were absent in all noninhibitory fractions (Fig. 1B and fig. S1D).

We determined the effect of synthetic spermine and spermidine on HIV-1 variants, which only differ in their V3 loop sequence determining the co-receptor tropism (*40*). The experiments were carried out with chemically defined medium and in the absence of fetal calf serum (FCS), which contains amine oxidases that convert polyamines into highly toxic intermediates (*41*, *42*). Under these conditions, both polyamines were not cytotoxic for TZM-bl and primary $CD4^+$ T cells (fig. S3, A and B). Spermine and spermidine selectively inhibited the four analyzed X4-HIV-1 variants with a mean 50% inhibitory concentration (IC_{50}) of 0.66 ± 0.14 mM (Fig. 1C and fig. S4) and 1.76 ± 0.55 mM (Fig. 1D), respectively, while infection of five R5-HIV-1 clones was not affected (Fig. 1, C and D). Similarly, spermine had no inhibitory effect on nine analyzed R5 T/F HIV-1 clones (Fig. 1E) and only completely inhibited a dual-tropic HIV-1 variant when combined with the CCR5 antagonist maraviroc (fig. S5). Putrescine and ornithine (fig. S1D), two other polyamines naturally present in semen at lower concentrations, had no effect on X4 virus infection (fig. S6, A and B).

Mechanistical studies showed that treatment of target cells, but not of virions, with spermine or spermidine prevented X4-HIV-1 infection (Fig. 1, F and G). Time-of-addition experiments further revealed that spermine only efficiently blocked X4 infection when added before or simultaneously with the virus (Fig. 1H) but not if added 2 hours after infection (Fig. 1I). Thus, spermine and spermidine inhibit X4-HIV-1 by targeting the cells. As semen is a protein-rich body fluid, we also analyzed whether spermine is active in the presence of albumin. As shown in fig. S6C, albumin concentrations of up to 50 mg/ml did not abrogate the anti-X4 activity of spermine.

Spermine inhibits infection of primary cells with X4-HIV-1

Next, we analyzed whether spermine may also inhibit viral infection of primary $CD4^+$ T cells and again observed a concentration-dependent reduction of X4-tropic HIV-1 but not R5-tropic HIV-1 infection (Fig. 2A). While HIV-1 infection with cell-free viral particles has been largely documented, the virus may also be transmitted by direct cell-to-cell contacts (*43*, *44*). Thus, we further analyzed whether spermine may inhibit cell-to-cell transfer of X4 and R5 primary HIV-1 strains from infected T cells to noninfected $CD4^+$ T cells or monocyte-derived macrophages. Spermine selectively reduced X4-HIV-1 but not R5-HIV-1 cell-to-cell transfer in both coculture experimental systems (Fig. 2, B and C). Because HIV-1 cell-to-cell transfer from infected $CD4^+$ T cells toward macrophages is mainly related to a cell-cell fusion process leading to the formation of virus-productive multinucleated giant cells (MGCs) (*45*, *46*), we also analyzed spermine activity by evaluation of MGC formation. Spermine specifically inhibited X4 viruses′ induction of MGCs, while R5 viruses still productively infected macrophages (Fig. 2, D to F). Transfer of dual-tropic HIV-1 89.6 from T cells to macrophages was only inhibited by a combination of spermine and maraviroc, while both substances alone had no effect (fig. S7, A to C). Together, spermine inhibits not only cell-free but also cell-associated X4-HIV-1 infection of primary $CD4^+$ T cells and macrophages.

Spermine interacts with the binding pocket of CXCR4

To analyze whether spermine directly binds CXCR4, we performed Gaussian accelerated molecular dynamics (GaMD) simulations, in which the spermine molecule was allowed to freely approach the CXCR4 receptor without binding bias (see computational details). The crystal structure of CXCR4 revealed that the binding pocket is open and negatively charged and can be separated into a major and minor pocket (*47*). The potential of mean force (PMF) obtained from the analysis of the trajectories indicated that spermine adopts binding poses targeting both binding pockets of CXCR4 (Fig. 3A). Furthermore, the analysis of the trajectories revealed three most populated clusters of structures, which together comprise more than 85% of the total sampling (Fig. 3B). The assessment of the intermolecular interactions in the corresponding representative structures evidences the key role of the amino groups of spermine, especially in the primary amines, in binding to CXCR4. These groups establish strong interactions with acidic residues at the binding region of CXCR4, notably D262, E277, D187, and E288 (Fig. 3B and figs. S8 and S9). The primary amines of spermine are in all cases involved in interactions with the receptor, although the remaining amino groups of spermine also contribute to the binding. Accordingly, the double acetylation at the primary amines should decrease the binding to the receptor, even if the conformational flexibility of this molecule will allow for new contacts via the remaining groups. Thus, our computational models also suggest that a spermine molecule that is fourfold acetylated should exhibit none to very poor binding to CXCR4.

To experimentally prove the interaction of spermine with CXCR4, we carried out surface plasmon resonance (SPR) spectroscopy with the receptor being immobilized on a sensor chip, as described (*48*). We found that spermine resulted in a concentration-dependent binding that was detected at concentrations as low as 1 μM (fig. S10, A and B). These results were confirmed by an alternative SPR-based approach in which virus-like particles expressing

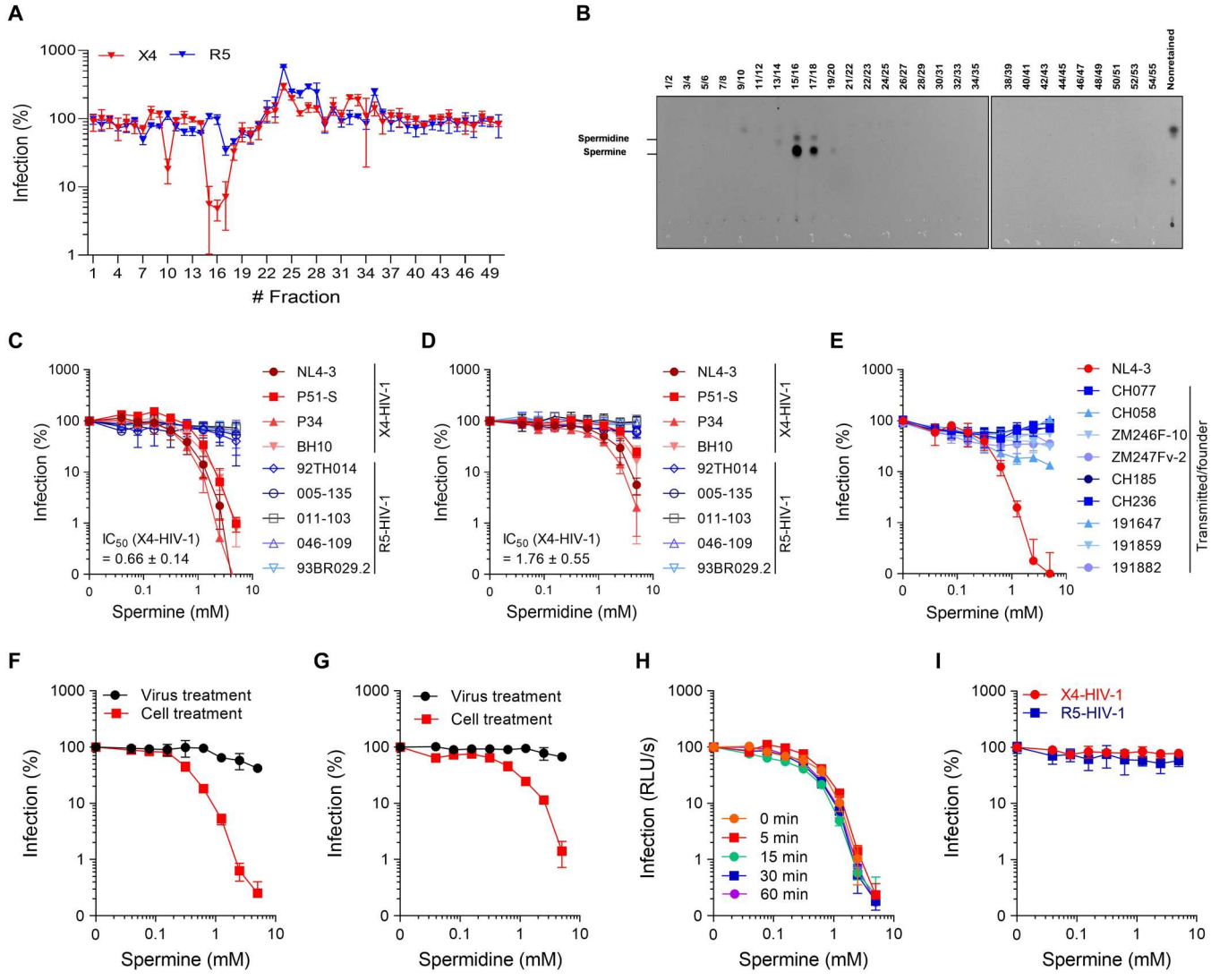

Fig. 1. Identification of spermine and spermidine as inhibitors of X4-HIV-1. (**A**) Identification of chromatographic fractions (from Source 15RPC) of an SP-derived compound library that inhibit X4-HIV-1 but not R5-HIV-1 infection. Fractions were added to TZM-bl cells and infected with X4-HIV-1 or R5-HIV-1. X4-HIV-1–inhibiting fractions 15 to 18 were shown to contain spermine and spermidine (see fig. S1). (**B**) TLC plate image showing separation of dansyl-derivatized (see fig. S2A) fractions (two pooled per lane) in cyclohexane:ethyl acetate (2:3, v/v). (**C** and **D**) Effect of **s**ynthetic spermine (C) and spermidine (D) on X4-HIV-1 and R5-HIV-1 infection. TZM-bl cells were preincubated for 1 hour with spermine or spermidine and infected with X4-HIV-1 or R5-HIV-1 NL4-3 V3 loop variants. (**E**) Effect of spermine on R5 T/F HIV-1 infection of TZM-bl cells. (**F** and **G**) Spermine targets a cellular factor involved in X4-HIV-1 entry. TZM-bl cells or X4-HIV-1 were incubated for 1 hour with indicated concentrations of spermine (F) or spermidine (G). Thereafter, cells were infected with either X4-HIV-1 (cell treatment) or virions/polyamine mixtures and inoculated on TZM-bl cells, thereby diluting spermine 10-fold (virion treatment). (**H** and **I**) Spermine was added 0 to 60 min before infection with X4-HIV-1 (H) or 2 hours after infection with X4-HIV-1 or R5-HIV-1 (I) of TZM-bl cells. RLU, relative light units. For all experiments, infection rates were measured 2 days after infection by β-galactosidase assay. Values shown represent mean values of one (A, B, E, and H) or three (C, D, F, G, and I) experiments performed in triplicates ± SD.

CXCR4 (VLP-CXCR4) bind to a biotinylated form of spermine immobilized on a streptavidin-coated sensor chip. Moreover, a 15-min preincubation of the VLP-CXCR4 with different concentrations of free spermine before injection reduced their binding to the biotinylated spermine in a dose-dependent manner (fig. S10, C and D).

Having established that spermine directly binds CXCR4, we next analyzed the impact of spermine acetylation for receptor interaction. For this, we took advantage of a CXCR4 antibody competition assay that allows monitoring of receptor-ligand interaction (*49*). Spermine competed with the CXCR4 12G5 antibody, which binds close to the orthosteric binding pocket of the receptor, in a concentration-dependent manner (IC_{50} of 0.4 mM in SupT1 cells) (Fig. 3D). Spermine did not compete with the 1D9 control antibody, which binds to the CXCR4 N terminus, or a CD4 or CCR5 antibody (fig. S11, A and B), suggesting that spermine does not unspecifically interfere with antibody binding or bind to the other main HIV-1 (co)receptors. Two- and fourfold acetylated spermine (Fig. 3C) competed with the 12G5-CXCR4 antibody much less efficiently (Fig. 3D), as predicted by the computational studies. HIV-1 infection experiments showed that a twofold acetylation resulted in an eightfold attenuation of antiviral activity (IC_{50}, 2.3 mM), as compared to unmodified spermine (IC_{50}, 0.28 mM), whereas the

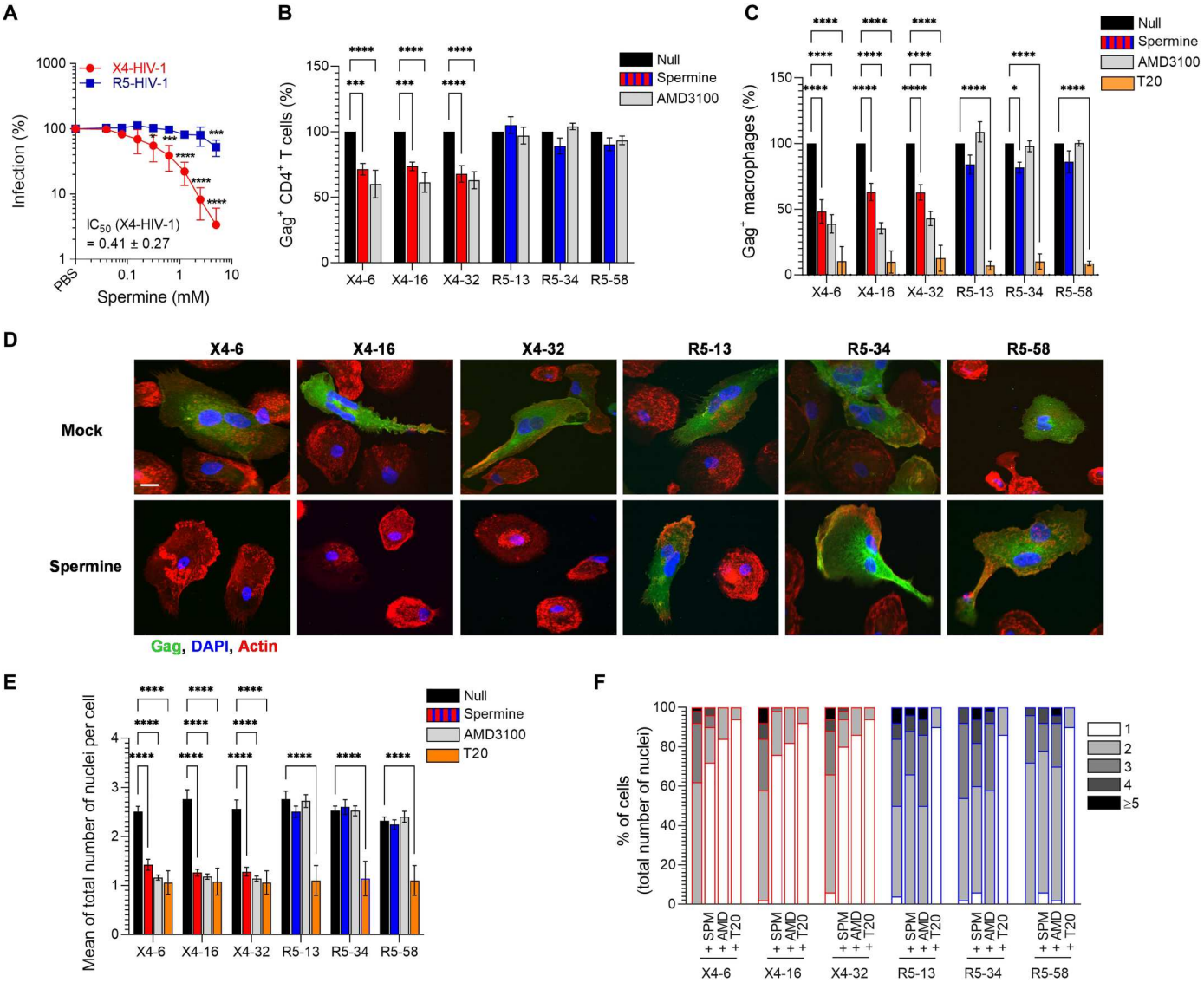

Fig. 2. Spermine inhibits X4-HIV-1 in primary cells. (**A**) Effect of spermine on HIV-1 infection of $CD4^+$ T cells. Activated primary $CD4^+$ T cells supplemented with spermine were infected with X4-HIV-1 or R5-HIV-1. Infection rates were determined by staining of p24 capsid protein and analysis in flow cytometry. Means derived from three individual experiments performed in triplicates are shown. (**B** to **F**) Effect of spermine on HIV-1 transmission from $CD4^+$ T cells to $CD4^+$ T cells (B) or monocyte-derived macrophages (MDMs) (C to F). Jurkat cells infected with the indicated X4 (X4-6, X4-16, and X4-32) or R5 (R5-13, R5-34, and R5-58) primary viruses were cocultured for 6 or 24 hours with primary $CD4^+$ T cells or macrophages pretreated or not (null) with spermine (0.6 mM), AMD3100 (5 μM), or T20 (5 μM). (B and C) Percentage of Gag^+ $CD4^+$ T cell and macrophage targets was determined by flow cytometry. Means of at least four independent experiments of at least six different donors are shown. (D to F) After coculture, Jurkat cells were eliminated by extensive washings, and MDMs were stained with anti-Gag (green), phalloidin (actin, red), and 4′,6-diamidino-2-phenylindole (DAPI) (nuclei, blue) for confocal microscopy. Representative images are shown in (D). Scale bar, 10 μm. The total number of nuclei ($DAPI^+$) per Gag^+ MDM was quantified from images on at least 50 cells. In (E), results are expressed as the mean nucleus number per Gag^+ MDM. In (F), results are expressed as the percentages of Gag^+ MDMs. Representative means of at least four independent experiments performed with MDMs from at least four different donors ± SEM are shown. $^*P < 0.05$; $^{**}P < 0.01$; $^{***}P < 0.001$; $^{****}P < 0.0001$. (A) One-way analysis of variance (ANOVA), Sidak's multiple comparison test. (B, C, and E) Two-way ANOVA, Turkey's multiple comparison test. SPM, spermine; AMD, AMD3100; red, X4-HIV-1; blue, R5-HIV-1.

fourfold acetylated molecule was entirely inactive in preventing X4-HIV-1 infection (Fig. 3E). Although results clearly show that the amine groups in spermine are essential for CXCR4 binding and inhibition of X4-HIV-1 infection, we noticed the discrepancy between both assays. The observed variations can be attributed to the unique characteristics of the two experimental systems. In the antibody competition assay, binding of a CXCR4-specific antibody is impeded. Conversely, during HIV-1 infection, the viral glycoprotein gp120 initially binds to CD4, resulting in conformational changes in gp120 and exposure of the V3 loop. Subsequently, the V3 loop interacts with the co-receptor CXCR4, a process that is inhibited by spermine. Therefore, the disparities in binding kinetics, affinities, and modalities between the two ligands—the antibody and gp120—could influence the assay results. The quadruple-

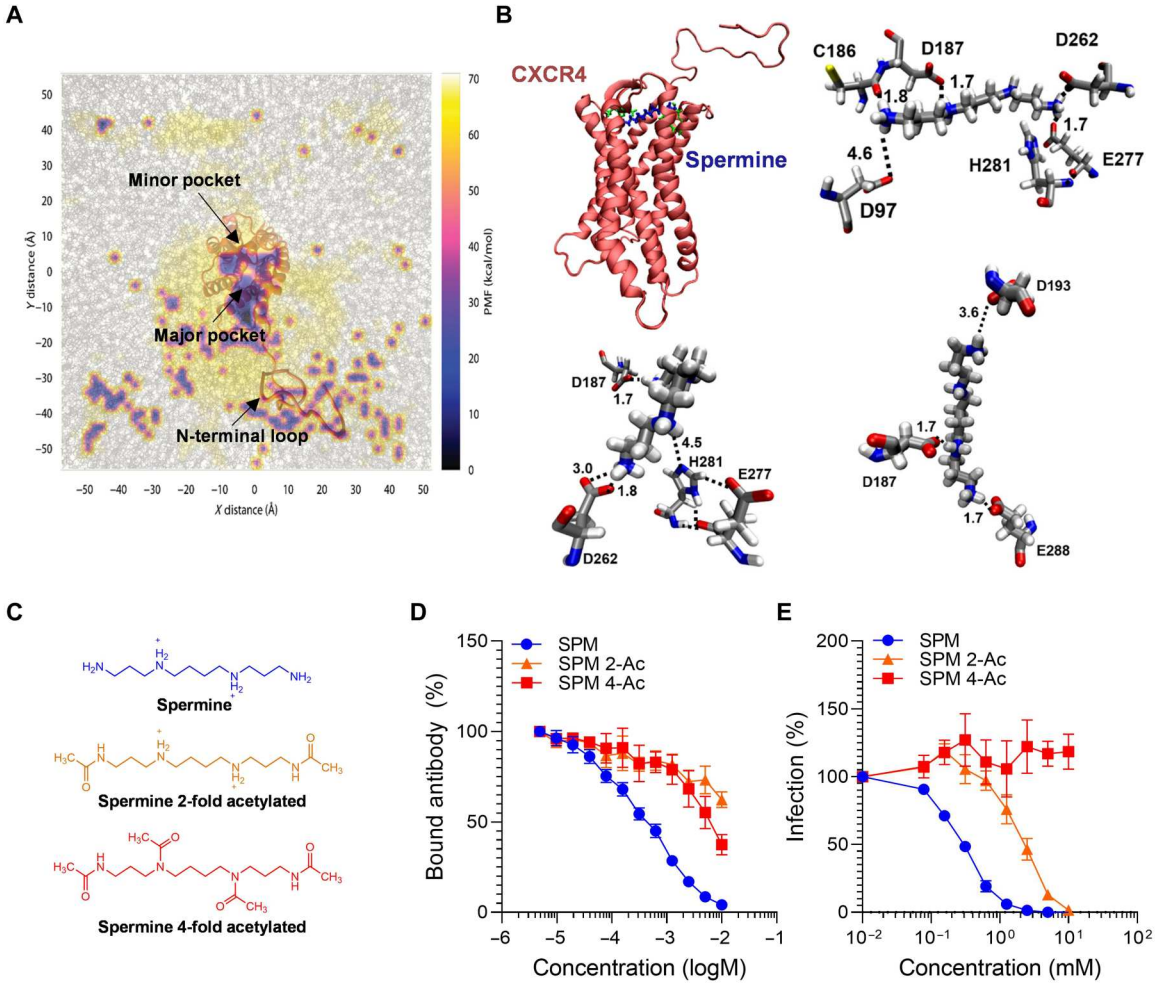

Fig. 3. Spermine binds to CXCR4 and competes with a CXCR4 antibody. (**A**) Top view of CXCR4 embedded in a lipid membrane. The view is superimposed by the PMF derived from GaMD simulations, which displays two main binding sites (deep blue) involving residues of both the major and minor binding pockets of CXCR4. (**B**) Representative structures of the most populated binding motifs of spermine evidence the conformational flexibility of spermine as well as the key role in binding of its amino groups, especially the primary. Representative distances are shown. Figure S9 shows an overlay of the binding poses. Top left: One of the binding poses. Red, CXCR4; blue, spermine; green, residues interacting with spermine. (**C**) Chemical structure of spermine and its two- and fourfold acetylated derivatives. (**D**) Competition of unmodified, two- and fourfold acetylated spermine with 12G5 antibody for binding to CXCR4. CXCR4-expressing SupT1 cells were incubated with increasing concentrations of compounds in the presence of a constant concentration of a CXCR4 antibody (clone 12G5) at 4°C for 2 hours. Bound antibody was determined by flow cytometry. Data derived from at least three individual experiments ± SEM are shown. (**E**) Effect of spermine and acetylated variants on X4-HIV-1 infection. TZM-bl cells were preincubated with compounds for 60 min before they were inoculated with X4-HIV-1. Infection rates were determined after 2 days by β-galactosidase assay. Data derived from three individual experiments performed in triplicates ± SEM are shown.

acetylated spermine retains some affinity toward CXCR4, triggering antibody competition. However, this affinity may be insufficient to inhibit HIV-1.

To further investigate the binding poses of spermine within the CXCR4 binding pocket, we introduced point mutations at those positions in the receptor that were predicted to interact with spermine (fig. S12, A to D). The respective alanine-CXCR4 mutants were transfected into 293T cells (with low endogenous CXCR4 levels) (fig. S12B), and the efficacy of spermine to dose-dependently compete with the 12G5 antibody was determined (fig. S12, C and D). As expected from the different binding modes of spermine, none of the point mutations abrogated spermine binding entirely (fig. S12, C and D). However, several mutations resulted in increased IC_{50} values, indicating a diminished spermine binding to specific CXCR4 residues. Mutations D187A and E277A reduced spermine binding most efficiently (fig. S12D) and represent the most contacted residues in the simulations (fig. S12A). These data largely confirm the computational predictions. Other residues such as I265, H281, I284, and E288 are also contacted but are comparatively less relevant for the binding of spermine to CXCR4. Only the mutation of D262 did not result in loss of activity. This can be attributed to the conformational flexibility of spermine, which allows compensating the loss of the interactions with D262 by establishing new contacts with nearby residues.

Furthermore, molecular docking calculations revealed that putrescine and ornithine bind less efficiently than spermine to CXCR4 (fig. S13, A and B). Putrescine and ornithine are smaller, less positively charged with respect to spermine, and establish

weaker interactions with the binding site of CXCR4. In the case of ornithine, the carboxyl group could introduce repulsive interactions with the acidic residues at the binding pockets of CXCR4. Experimentally, both ornithine and putrescine did not compete with the CXCR4 antibody (clone 12G5) (fig. S13, C and D), explaining the lack of X4-HIV-1 inhibition (fig. S6, A and B), in accordance with the computational results.

SP selectively inhibits X4-tropic HIV-1

Spermine is the most abundant polyamine in SP with concentrations between 2 and 14 mM (*50*, *51*). TLC of individual SP samples confirmed this concentration range (3.2 to 10.6 mM), with a median spermine concentration of 3.8 mM (table S2). The analysis of endogenous spermine required to study the effects of SP on viral infection is, however, hampered by the well-known cytotoxic effects of this body fluid. SP cytotoxicity is caused by conversion of seminal polyamines through di-amine oxidases present in FCS, a cell culture supplement (*41*, *52*, *53*), and SP itself. To minimize SP toxic effects, we combined the use of serum-free medium as used for synthetic polyamines above (fig. S3, A and B) with addition of the amine oxidase inhibitor aminoguanidine (*41*). As shown in (*41*) and fig. S14, these conditions allow to study SP concentrations of up 50 volume percent (volume %) without causing confounding cytotoxic effects. However, due to the high viscosity of the SP at 50 volume %, this concentration was excluded from further experiments.

To determine the effect of SP on X4-HIV-1 and R5-HIV-1 infection, individual SP samples were added to cells at concentrations up to 25 volume %. After 1 hour of incubation, cells were infected by spinoculation with normalized X4-HIV-1 and R5-HIV-1. Infection rates were determined 2 days later, showing that all SP samples inhibited X4-HIV-1 in a concentration-dependent manner, with a mean IC_{50} of only ~5.3 volume % (corresponding to ~0.26 mM of spermine) (Fig. 4A, left). No inhibitory but rather an enhancing effect of SP was observed for R5-HIV-1 infection at low volume % of SP (Fig. 4A, right). This enhancing activity of SP is mediated by positively charged peptide fibrils in semen, such as the semen-derived enhancer of viral infection (SEVI), but usually more pronounced at low infectious doses (*54*–*56*). Thus, we finally evaluated whether spermine may restrict SEVI-treated X4 and R5 viruses. SEVI increased X4 and R5 infection by 8- and 12-fold, as previously published (*55*), and spermine almost completely blocked infection of SEVI-treated X4-HIV-1, while R5-HIV-1 was not affected (Fig. 4B and fig. S15).

DISCUSSION

Collectively, our findings demonstrate that spermine and spermidine are noncanonical ligands of CXCR4 and specific inhibitors of X4-HIV-1 infection. Spermine and spermidine are naturally present in semen, with spermine concentrations reaching up to 14 mM (*39*). These concentrations are sufficient to inhibit X4-HIV-1 infection of cell lines and primary $CD4^+$ T cells, and to efficiently reduce X4 virus transmission from infected T cells to noninfected T cells or macrophages. We also show that physiologically relevant concentrations of SP restrict X4-HIV-1 while enhancing R5-HIV-1 infection and—in agreement with these findings—that spermine also inhibits fibril-exposed X4 but not R5 viruses. Because HIV-1–containing semen is an important vector for viral transmission, the presence of an abundant and specific inhibitor of X4 viruses (and the absence of inhibitors of R5 virus) provides a very plausible explanation for the very rare cases of X4 virus transmission. Thus, spermine and perhaps other polyamines in SP are likely to represent the long-sought gate keepers that restrict sexual X4-HIV-1 transmission.

Spermine and spermidine bind CXCR4 and presumably block the interaction of the gp120 V3 loop region of X4-HIV-1 with its co-receptor, preventing subsequent rearrangements in gp41, and consequently membrane fusion and infection. Our computational model suggests that spermine interacts with the whole binding region of CXCR4, overlapping with the binding regions of X4-gp120 V3 to CXCR4 (*57*). The model further suggests that the

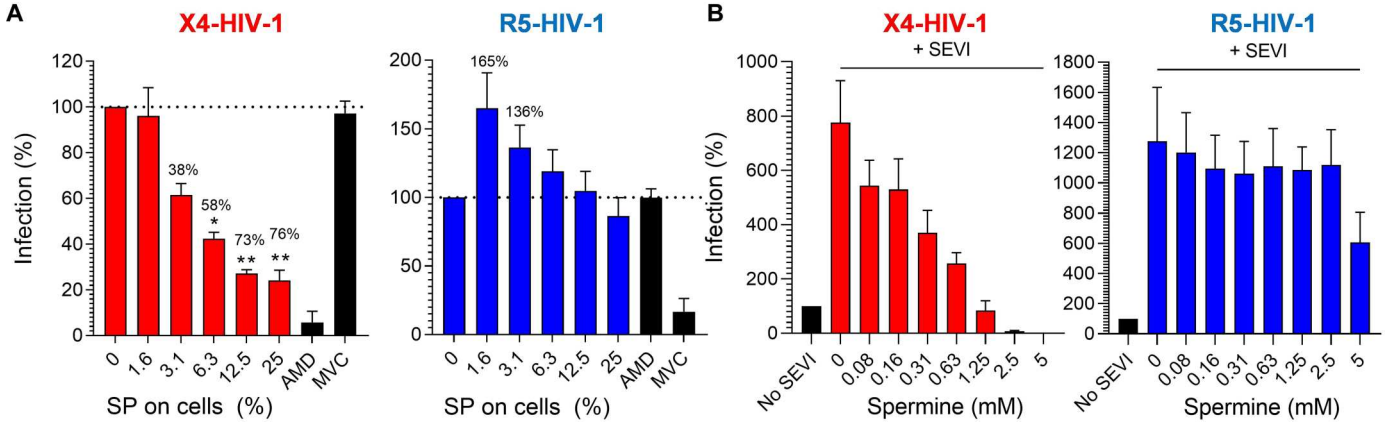

Fig. 4. Seminal plasma specifically blocks X4- and not R5-HIV-1 infection. (**A**) TZM-bl cells were treated with indicated concentrations (volume %) of fresh SP derived from single donors. One hour later, X4-HIV-1 or R5-HIV-1 was added and spinoculated for 30 min. Inoculum was removed 2 hours later, and infection rates were determined after 2 days. Values shown are mean values from eight individual experiments performed in triplicates ± SEM. (**B**) Effect of spermine on SEVI-exposed X4 and R5 virus. TZM-bl cells were pretreated with indicated spermine concentrations for 1 hour and inoculated with SEVI/PBS-treated X4-HIV-1 or R5-HIV-1. Infection rates were determined 2 days later. Means derived from three individual experiments performed in triplicates ± SEM are shown. *$P < 0.1$, **$P < 0.01$, ***$P < 0.001$, and ****$P < 0.0001$ compared to control without SP (A) or +SEVI without spermine (B) (one-way ANOVA, Dunnett's multiple comparison test). AMD, AMD3100; MVC, maraviroc; SEVI, semen-derived enhancer of viral infection; ns, not significant; red, X4-HIV-1; blue, R5-HIV-1.

spermine/CXCR4 interaction is mainly established by the four positively charged amino groups of the polyamine, also providing an explanation for the comparable lower antiviral efficacy of spermidine (only three amine groups), putrescine, ornithine, and the acetylated spermine derivatives. Mutational analyses, antibody competition, and HIV-1 infection experiments confirmed the computational predictions, showing a reduced CXCR4 binding affinity and antiviral activity of the acetylated spermine derivatives. Furthermore, point mutations in the binding site of CXCR4 demonstrate the relevance of acidic residues as they are the most contacted residues with an impact on the binding of the spermine. SPR spectroscopy confirmed interaction of spermine with CXCR4, however, leaving open the possibility that more than one spermine can bind to CXCR4. Despite the flexibility of the molecule in the binding pocket of CXCR4, modeling data show that it is unlikely for more than one spermine molecule to bind simultaneously into the binding cavity of CXCR4. However, less conserved interactions with the N-terminal region of the receptor could be established.

High spermine concentrations in semen may explain restriction of X4-HIV-1 and thus selective transmission of R5 viruses in scenarios involving virus-containing semen, such as male-to-female or male-to-male transmissions. However, our findings cannot explain the apparent similar selective sexual transmission bias of R5 viruses from female to male or by other routes of infection. Thus, although the presence of a highly concentrated CXCR4 binder and selective X4-HIV-1 inhibitor most likely influences sexual transmission events involving semen, it may not be the sole determinant for bottlenecking virus transmission and other, yet to be identified, factors most likely contribute as well.

Spermine and spermidine are produced in the prostate gland and play a critical role in protecting and nourishing spermatocytes. Their antioxidant and nutritional properties are crucial for maintaining the health and viability of sperm, and they contribute to the success of fertilization and reproduction (*58*). Whether spermine/spermidine interactions with CXCR4 further result in receptor signaling and cellular responses remains to be clarified. In this context, it should be noted that the immunosuppressive and anti–type I interferon function of positively charged monoamines has been linked to CXCR4 engagement (*59*, *60*), suggesting that spermine and spermidine might exert similar functions upon deposition in the female reproductive tract.

MATERIALS AND METHODS

Reagents

Spermine, spermine tetrahydrochloride and spermidine, putrescine, and ornithine were obtained from Sigma-Aldrich and dissolved in H_2O. AMD3100 (Plerixafor) and maraviroc were obtained from Sigma-Aldrich and dissolved in H_2O or dimethyl sulfoxide (DMSO), respectively. Aminoguanidine was obtained from Sigma-Aldrich and diluted in phosphate-buffered saline (PBS) before it was supplemented into cell culture medium. TLC plates, solvents, and reagents for dansyl derivatization were purchased from Sigma-Aldrich. T20 was obtained from the AIDS Research and Reference Reagent Program, Division of AIDS, National Institute of Allergy and Infectious Diseases.

Semen and SP

Semen was obtained from adult donors with informed consent by ejaculation and allowed to liquefy for 30 min. To obtain a larger sample volume, two to three samples were pooled at a time and centrifuged at 14,000*g*. The resultant supernatant (SP) was used for infection experiments.

Ethics statement

All experiments and methods were performed in accordance with relevant guidelines and regulations. Experiments involving semen were reviewed and approved by Ethics Committee of Ulm University (file references 88/17, 200/17). Informed consent was obtained from all human subjects. All human-derived samples were anonymized before use. For isolation of primary T cells and monocytes, blood samples from anonymous healthy donors were purchased at "Etablissement Français du Sang" (EFS; the French National Blood Agency, Paris-Saint-Antoine-Crozatier, Paris, France). Samples used for scientific purposes were carried out in accordance with convention between EFS and Inserm. Donors provided written informed consent to EFS at the time of blood collection.

Generation of a compound library from SP

SP-derived libraries were provided by the Ulmer Zentrum für Peptipharmazeutika, Ulm. Two milliliters of SP was filtered by ultrafiltration [Amicon Ultra, molecular weight cutoff (MWCO) of 30 kDa] and washed five times with PBS. The M < 30 kDa filtrate was spiked with 0.1% heptafluorobutyric acid (HFBA) and applied to a Source 15RPC (polystyrene/divinyl benzene matrix) reversed-phase column (GE Healthcare Life Science, USA) of dimensions 1 cm by 12.5 cm, previously equilibrated with solvent A, 0.1% HFBA (HPLC grade, Thermo Fisher Scientific, USA) in water. Elution was performed at 2 ml/min, from 0% B to 80% B in 60 min, being A, 0.1% HFBA in water, and B, 0.1% HFBA in acetonitrile (HPLC grade, J.T.Baker, USA). Eluting compounds were detected online by ultraviolet absorption at 280 nm. Fractions were collected every 1 min and evaporated in a vacuum concentration system. The chromatographic equipment used for separation was a Shimadzu LC-10Avp series HPLC system (Shimadzu, Japan).

Mass spectrometry analysis

A 10-µl aliquot of the fraction was diluted with 10 µl of 2% formic acid/98% acetonitrile and analyzed by static infusion into an LTQ Orbitrap Velos Pro system (Thermo Fisher Scientific). Spectra were acquired using the orbitrap part of the instrument at a resolution of 30,000. For visualization, XCalibur Qual Browser (Thermo Fisher Scientific) was used. The experimental monoisotopic masses of spermine and spermidine were compared to the values available at PubChem 2.1 (https://pubchem.ncbi.nlm.nih.gov/compound/Spermine and https://pubchem.ncbi.nlm.nih.gov/compound/Spermidine).

Quantification of seminal polyamines by TLC

For quantification of polyamines in SP, samples were first diluted fivefold with PBS to obtain values in the linear range and spiked with a defined concentration of 1,7-diaminoheptane to estimate polyamine recovery. Diluted samples were de-proteinized by incubating with an equal volume of 4% trichloroacetic acid (5 min, 37°C, shaking) followed by centrifugation (10,000 rpm, 1 min) to pellet the denatured proteins. Alternatively, ultrafiltration (Amicon

Ultra, MWCO of 3 kDa) was performed. Fifty microliters of saturated Na_2CO_3 solution was added to an equal volume of de-proteinized sample to adjust the pH. Polyamine derivatization was then carried out by adding 100 µl of dansyl chloride solution (5 mg/ml in acetone, HPLC grade) and incubating at 37°C for 2 hours while shaking. Excess dye was removed by adding 25 µl of L-proline solution (150 mg/ml in H_2O) and incubating for an additional 30 min. Afterward, 100 µl of toluene was added and samples were vortexed and briefly centrifuged. The organic layer containing the dansylated polyamines was then extracted. For TLC, 1 to 3 µl of extracted dansylamines were spotted on silica gel plates (60-Å pore size) with fixed-volume microcapillary glass pipettes (Drummond Microcaps). Chromatographic separation was then performed in cyclohexane/ethyl acetate (2:3). After drying, plates were imaged in a Gel Doc XR+ system and densitometric quantification of spots was performed with Fiji.

Cell culture

Adherent TZM-bl reporter cells containing the lacZ reporter genes under the control of the HIV LTR (long terminal repeat) promoter and stably expressing CCR5 were obtained from the National Institutes of Health (NIH) AIDS Reagent Program (catalog number 8129), and 293T cells were obtained from the American Type Culture Collection (ATCC) (CRL-11268). Both were cultured in Dulbecco's modified Eagle medium (DMEM) supplemented with 10% FCS, penicillin (100 U/ml), streptomycin (100 µg/ml), and 2 mM L-glutamine (Gibco). SupT1 cells and Jurkat cells were obtained from ATCC (CRL-1942 and TIB-152, respectively) and cultured in RPMI 1640 (Gibco) supplemented with 10% FCS, penicillin (100 U/ml), streptomycin (100 µg/ml), and 2 mM L-glutamine (Gibco). Human $CD14^-CD4^+$ T cells from healthy male and female blood donors were prepared by negative selection using the RosetteSep $CD4^+$ T cell enrichment cocktail according to the manufacturer's instructions and subsequent Ficoll density centrifugation and activated for 3 days in RPMI 1640 medium (Gibco) containing 10% FCS, penicillin (100 U/ml), streptomycin (100 µg/ml), 2 mM L-glutamine, interleukin 2 (10 ng/ml), and phytohemagglutinin (1 µg/ml). Monocytes were purified from blood of healthy donors using a CD14-positive selection kit (CD14 microbeads, Miltenyi) according to the manufacturer's guidelines and then differentiated into macrophages [monocyte-derived macrophages (MDMs)] for 8 days in RPMI 1640 culture medium supplemented with 10% FCS, antibiotics, and 25 ng/ml of granulocyte-macrophage colony-stimulating factor (GM-CSF) and macrophage colony-stimulating factor (M-CSF) (Miltenyi). Experiments in the presence of polyamines were performed in chemically defined X-VIVO 15 medium (Lonza). Experiments in the presence of SP were performed in X-VIVO 15 medium supplemented with 0.05 mM aminoguanidine as described before (*41*) and gentamicin (50 µg/ml).

Cell viability

The cytotoxic effects derived from spermine and spermidine or SP were analyzed using the MTT [3-(4,5-dimethylthiazole-2-yl)-2,5 diphenyltetrazolium bromide] assay under experimental conditions corresponding to those used in the respective infection assays. After incubation time, 20 µl of MTT (Sigma-Aldrich, #M2003) solution (5 mg/ml) was added to cells. After 3 hours, the cell-free supernatant was removed and the formazan crystals that have been formed on living cells were dissolved in 100 µl of DMSO-ethanol (1:1). Optical density was detected at 490/650 nm.

Virus stock preparation

Viral stocks of R5-tropic and X4-tropic HIV-1 NL4-3–derived V3 variants (*40*), as well as HIV-1 virions pseudotyped with the envelope glycoproteins from different T/F viruses (*14*) were generated by transient transfection of 293T cells with proviral DNA as described (*54*). After overnight incubation, the transfection mixture was replaced by 2 ml of DMEM containing 2.5% FCS. After another 24 hours, the cell-free and virus-containing supernatant was harvested and centrifuged to remove cell debris. Aliquots were stored at −80°C. For infection of primary cells, the supernatant was 10-fold concentrated by ultrafiltration (Amicon, MWCO of 100 kDa) and resuspended in X-VIVO 15 medium.

Infection of TZM-bl cells in the presence of SP library fractions or polyamines

To examine the influence of polyamines on X4-tropic and R5-tropic HIV-1 infection, 1×10^5 TZM-bl cells/ml were seeded into 96-well flat-bottom plates (100 µl). The next day, the medium was changed to 170 µl of X-VIVO 15 chemically defined medium (Lonza) and 20 µl of substances was added. TZM-bl cells were incubated for 1 hour at 37°C before they were inoculated with 10 µl of virus (cell treatment). Alternatively, the virus was treated for 15 min with the polyamines before 20 µl of the mixture was added to TZM-bl cells in 180 µl of X-VIVO 15 medium, thereby diluting the mixture 10-fold. To analyze SP-derived library fractions, TZM-bl cells in 85 µl of X-VIVO 15 medium were preincubated with 5 µl of the respective fraction. Cells were inoculated with 10 µl of virus after 30 min. Infection rates were measured 2 days after infection using a Gal-Screen system (Applied Biosystems).

Infection of $CD4^+$ T cells in the presence of polyamines

Isolated and activated $CD14^-CD4^+$ T cells were seeded at a density of 2×10^5 cells per well in 96-well flat-bottom plates. Cells were preincubated with compounds in 190 µl of medium for 1 hour and then infected with 10 µl of 10-fold concentrated X4-tropic NL4-3 or R5-tropic transmitted founder CH068. Infection rates and viability were determined 2 days after infection by p24 staining as described previously (*61*) and fixable viability stain 660 (BD Horizon) and analyzed by flow cytometry.

Infection of TZM-bl cells in the presence of SP

To examine the inhibition effect of human SP on HIV-1 infection, 1×10^5 TZM-bl cells/ml were seeded into 96-well flat-bottom plates (100 µl). The next day, the medium of the cells was replaced by X-VIVO 15 chemically defined medium (Lonza) supplemented with 0.05 mM aminoguanidine (*41*) and gentamicin (50 µg/ml). SP diluted in PBS was added to cells and incubated for 1 hour at 37°C. After incubation, cells were infected with X4-tropic or R5-tropic HIV-1 by spinoculation (30 min, 2090*g*, 37°C) and incubated for another 2 hours. Final inoculum was discarded, cells were washed with PBS, and 200 µl of X-VIVO 15 medium [+ 0.05 mM aminoguanidine, gentamicin (50 µg/ml)] was added. Infection rates were measured 2 days after infection using a Gal-Screen system (Applied Biosystems).

Infection experiments in the presence of SEVI

PAP248-286 was purchased from Celtek Peptides. SEVI was prepared by dissolving the peptide at 2.5 mg/ml in PBS and shaking at 2000 rpm on a rotary shaker for 2 days at 37°C. For infection experiments, 1×10^5 TZM-bl cells/ml were seeded into 96-well flat-bottom plates (100 μl). The next day, the medium was changed to 170 μl of X-VIVO 15 chemically defined medium (Lonza) and 20 μl of substances was added for 1 hour. The virus was 1:1 mixed with SEVI or PBS and preincubated for 10 min at room temperature before cells were inoculated with 10 μl of the mixture. Infection rates were measured 2 days after infection using a Gal-Screen system (Applied Biosystems).

Cell-to-cell infection assays

For cell-to-cell virus infection assays between $CD4^+$ T cells and infected $CD4^+$ T cells to MDMs, human Jurkat $CD4^+$ T cells were infected with VSVg-pseudotyped virus stocks at a multiplicity of infection of 0.5 for 48 hours and then cocultured for 6 or 24 hours with primary $CD4^+$ T cells preloaded with the CellTrace dye or macrophages pretreated or not with spermine (0.6 mM), AMD3100 (5 μM), or T20 (5 μM). Cells were then stained with anti-Gag KC57 monoclonal antibody (Beckman Coulter), and the percentage of Gag^+ T cell and macrophage targets was determined by flow cytometry. To analyze virus cell-to-cell transfer to macrophages after coculture with infected T cells, MDMs were permeabilized and stained using KC57 fluorescein isothiocyanate (FITC)–conjugated anti-Gag antibody and phalloidin–Alexa Fluor 647 (Molecular Probes). Coverslips were then washed and mounted on slides using 10 μl of Fluoromount (Sigma-Aldrich). Images were acquired on a spinning disk (CSU-X1M1, Yokogawa)–equipped inverted microscope (DMI6000, Leica) and were then processed using Fiji software (ImageJ, NIH). Quantitative imaging analysis was performed using Fiji by defining a region of interest using the actin staining and measuring the whole fluorescence intensity of the Gag staining, with respect to noninfected cells. The number of $DRAQ5^+$ nuclei per MDM was determined from images of at least 100 cells, followed by processing using Fiji as described previously (Bracq, 2017, JVI).

Antibody competition assay

Competition of polyamines with receptor antibodies was performed as described previously (*49*). For this, compounds were serially diluted in cold PBS and added to CXCR4-expressing SupT1 or detached TZM-bl cells together with the respective fluorescently labeled antibodies [anti-CXCR4 clone 12G5–allophycocyanin, BD 555976; anti-CXCR4 clone 1D9–phycoerythrin (PE), BD 551510; anti-CD4 clone OKT4-BV605, BioLegend, #317438; and anti-CCR5 clone #45531-PE, R&D Systems, FAB182P100]. Cells were incubated at 4°C for 30 min before unbound antibody was removed by 2× washing with fluorescence-activated cell sorting buffer, and cells were analyzed via flow cytometry. The sample stained with the antibody and without compound (buffer control) was set to 100%, and the sample without the antibody was set to 0%. For each antibody, the respected isotype controls were used to remove background signal.

Site-directed CXCR4 mutagenesis and competition experiments

The human CXCR4 gene (isoform 1 or b, National Center for Biotechnology Information reference sequence: NP_003458.1, UniProtKB/Swiss-Prot: P61073-1) was amplified by polymerase chain reaction (PCR) of the pTrip_GFP_CXCR4 vector (provided by F. Bachelerie, Paris, France) by generating the flanking single cutter sites Nhe I and Hind III. The PCR fragment was ligated in the empty $pcDNA3.1^+$ vector (Life Technologies GmbH, Darmstadt). Afterward, the internal ribosomal entry site (IRES)–enhanced green fluorescent protein (eGFP) cassette of the proviral clone pBR_NL4-3_IRES-eGFP was PCR-amplified with Eco RI and Not I single cutter sites and ligated in the multiple cloning site after CXCR4. Site-directed mutagenesis (New England Biolabs, E0554S) was used to introduce different point mutations in this construct. As a negative control, a CXCR4 construct harboring two stop codons after the start codon and a mutation introducing a frameshift was cloned (mock control). Primers are listed in table S1.

Constructs were transfected into 239T cells. The next day, cells were detached and seeded into 96-V well plates (50,000 cells per well). Antibody competition assay was performed as described above using the CXCR4 antibody 12G5. In parallel, CXCR4 expression levels were determined by flow cytometry using the CXCR4 antibodies 12G5 and 1D9 and eGFP expression.

SPR spectroscopy with immobilized CXCR4

SPR was adapted from Boonen *et al.* (*48*). Donor plasmid for full-length CXCR4 with inserted T4 lysozyme sequence was obtained from DNASU plasmid repository as described (*48*). The protein contained a 10× histidine tag at the C-terminal end. High molecular weight recombinant bacmid containing the target gene sequence was prepared following Bac-to-Bac Baculovirus Expression System manual (Invitrogen). sf9 cells (1×10^6) were transfected by 6 μg of bacmid using 8 μl of CellFectin II reagent (Invitrogen) and Sf-900 II serum-free medium (Life Technologies) to generate recombinant baculovirus particles (P0 stock). Viral titer was increased by infecting 50 ml of sf9 cells at a density of 1.2×10^6 cells/ml, as determined on a LUNA-II Automated cell counter (Westburg, The Netherlands), with 2 ml of the P0 stock, and the suspension was allowed to grow for 72 hours at 27°C in a 250-ml shaking flask. Recombinant baculovirus particles were collected, filter-sterilized, and stored at 4°C (P1 stock). For CXCR4 expression, sf9 cells at a density of 1.2×10^6 cells/ml were infected with 3 ml of P1 virus and allowed to grow for 60 hours. When the cell viability dropped to 60 to 70%, cells were harvested by centrifugation at 200*g* and stored at −80°C until further use. CXCR4 (over)expression on the sf9 cells was verified by flow cytometry using CXCR4-specific antibody clone 12G5.

For membrane preparation, insect cells expressing CXCR4 on its membrane were disrupted in hypotonic buffer containing 20 mM Hepes (pH 7.5), 20 mM KCl, and 10 mM $MgCl_2$ as described previously (*48*). This was followed by dounce homogenization (25 strokes) to separate membrane sheets from soluble fraction. The membrane fraction was collected by ultracentrifugation at 80,000*g*, followed by washing (3×) in a buffer containing 50 mM Hepes (pH 7.5), 500 mM NaCl, and 10% glycerol to separate soluble and membrane-associated proteins from integral transmembrane proteins. The membrane fraction was resuspended in

solubilization buffer containing 20 mM tris (pH 7.0), 100 mM $(NH_4)_2SO_4$, 10% glycerol, 0.07% cholesteryl hemisuccinate (CHS), 0.33% *n*-dodecyl-β-D-maltopyranoside (DDM; Anatrace), 0.33% 3-[(3-cholamidopropyl)-dimethylammonio]-1-propane sulfonate (CHAPS; Anatrace), 0.33 mM 1,2-dioleoyl-*sn*-glycero-3-phosphocholine/1,2-dioleoyl-*sn*-glycero-3-phospho-*l*-serine (DOPC:DOPS) mixed in 7:3 (w/w) ratio (Avanti), and protease inhibitor tablet (Roche). The suspension was briefly sonicated and placed on a rocker for 3 hours at 4°C, after which the solubilized fraction was collected by centrifugation at 16,000*g* for 30 min.

All biosensor experiments were performed on Biacore T200 (Cytiva, Uppsala, Sweden) using carboxymethylated dextran chips preimmobilized with nitrilotriacetic acid. The sample compartment temperature was kept at 15°C and the analysis temperature at 25°C for all SPR experiments. The running buffer used in the experiments was used as previously described: 50 mM Hepes (pH 7.0), 0.1% DDM, 0.1% CHAPS, 0.02% CHS, 50 nM DOPC:DOPS (7:3), and 3 μM EDTA (running buffer 1) (*48*). Immobilization of CXCR4 was performed using a standard nickel chelation procedure. First, the second channel of the chip was activated with a 60-s injection of 0.5 mM $NiCl_2$ at a flow rate of 10 μl/min. Afterward, the membrane fraction containing His-tagged CXCR4, diluted 1:4 in solubilization buffer, was immobilized onto this channel by a 33-s injection at a flow rate of 10 μl/min. The capture level for all experiments averaged around 600 resonance units (RU). The first channel was also activated with nickel and used as a reference surface. To validate the stable conformation of CXCR4, conformation-dependent purified mouse anti-human CD184 (CXCR4) clone 12G5 (BD Pharmingen) was flown over both surface channels. Stability was confirmed before proceeding with the experiment.

For the spermine experiment, CXCR4 was immobilized and a waiting period of 30 min was applied with running buffer flowing over the surface to get a stable surface by removing any unbound or weakly bound ligand. Afterward, spermine was injected at given concentrations. Spermine was injected at a flow rate of 30 μl/min for 120 s using multiple cycle kinetics. The surface was regenerated using a 60-s injection of 350 mM EDTA followed by a 60-s injection of 1 M imidazole and concluded by three 60-s injections of 50 mM NaOH. All regenerations were performed at 30 μl/min. Several buffer blanks were used for double referencing. The experiments were performed in triplicate.

SPR spectroscopy VLP-CXCR4

Experiments were performed on a Biacore 3000 instrument (GE Healthcare) of the Platform of Molecular Interactions of the Institute of Biology Paris Seine (Sorbonne University) using a high-affinity streptavidin sensor chip (Cytiva). The sample compartment temperature was kept at 15°C and the analysis temperature at 25°C for all SPR experiments. The running buffer used in the experiments was HBS-EP buffer [0.01 M Hepes (pH 7.4), 0.15 M NaCl, 3 mM EDTA, 0.005% (v/v) Surfactant P20] supplemented with bovine serum albumin (200 μg/ml). Immobilization of biotinylated spermine was performed using the streptavidin-biotin procedure recommended by the manufacturer. First, the second channel of the chip was activated with a 60-s injection of NaCl (1 M)/NaOH (50 mM) at a flow rate of 10 μl/min. Afterward, the biotinylated spermine, diluted in solubilization buffer at a final concentration of 10 μM, was immobilized onto this channel by a 7-min injection at a flow rate of 10 μl/min. The capture level for all experiments averaged around 140 RU. The first channel was also activated and used as a reference surface.

After the immobilization of the biotinylated spermine, a waiting period of 30 min was applied with running buffer flowing over the surface to get a stable surface by removing any unbound or weakly bound ligand. Afterward, VLP-CXCR4 (ACROBiosystems) was injected at a concentration of 100 nM. For competition experiments, VLP-CXCR4 were preincubated for 15 min with various concentrations of free spermine and then injected at a flow rate of 2 μl/min for 300 s using multiple cycle kinetics. The surface was fully regenerated using a 15-s injection of 40 mM octyl glucoside, followed by a 15-s injection of 10 mM glycine-HCl (pH 1.5), and concluded by a 15-s injection of 1 M NaCl/50 mM NaOH. All regenerations were performed at 30 μl/min. Several buffer blanks were used for double referencing.

Molecular modeling

The initial simulation setup was built using the structure of CXCR4/EPI-X4 previously reported by us (*62*), with the EPI-X4 peptide removed and the CXCR4 receptor subsequently equilibrated. The CXCR4 receptor [Protein Data Bank (PDB) ID: 3ODU (*47*), with the N-terminal loop modeled based on the experimental structure with PDB ID: 2 K04 (*63*)] was embedded in a lipid membrane composed of 257 1-palmitoyl-2-oleoyl-sn-glycero-3-phosphocholine molecules. The solvent box comprised ~40,000 TIP3P (*64*) water molecules with 50 mM KCl. One spermine molecule was located in the bulk solvent, 20 Å away of the receptor′s site. The initial setup, without spermine, was generated using the CHARMM-GUI server (*65*–*67*) with the normal of the membrane plane fixed parallel to the *z* axis. The spermine molecule and the chloride counter ions were inserted in a second step by removing the water molecules within 2 Å of the spermine. A harmonic wall potential (100 kcal/mol per $Å^2$) was fixed 80 Å above the central plane of the membrane to prevent the spermine molecule from jumping between different sides of the bilayer via periodic boundary conditions. Energy minimization was performed on the initial system and subjected to a series of equilibration MD simulations before the GaMD runs (*68*). For the equilibration, harmonic position restraints with a force constant of 10 kcal/mol per $Å^2$ were applied on the protein atoms and the atoms of lipid head groups. The GaMD simulations were carried out using the equilibrated system. In all the cases, particle mesh Ewald (*69*) was used for the computation of long-range electrostatics. Short-range Lennard-Jones and electrostatic interactions were cut off at 12 Å; however, a switching function was used between 10 and 12 Å to smooth the interactions at the cutoff distance. Langevin dynamics was used with the temperature maintained at 300 K. The Langevin piston Nose-Hoover method (*70*, *71*) was used for maintaining the pressure at 1 atm. A time step of 2 fs was used for the integration of the equations of motion. The *z* coordinate of the center of mass of all lipids′ phosphate groups was subject to harmonic restraints (50 kcal/mol per $Å^2$), via steered dynamics with null velocity, to avoid translation of the membrane along the *z* axis. All the simulations were replicated three times using different initial random velocities. The CHARMM36 force field (*72*) in conjunction with the NAMD program version 2.13 (*73*) was used.

Dual-boost GaMD was carried out by applying boost potentials based on the total energy of the system and on the dihedrals′ contribution. The biasing potentials were equilibrated in two steps: first,

25 ns of classical MDs in which the potential energy distribution of the system is monitored. Then, during 50 ns, the biasing potential is equilibrated by fixing an energy threshold at the maximum value of the potential energy and successively updating this value after every step of the simulation. The constant of the harmonic bias was concurrently equilibrated by keeping the maximum SD of the biasing potential at 6 kcal/mol. Three replicas of GaMD simulations were performed by initializing the simulations with different random velocities. The production runs were extended to 350/325/300 ns, thus collecting a combined sampling of ~1 μs.

The reweighted PMF (*74*) from this sampling was obtained using the PyReweighting toolkit of Miao *et al.* (*75*). This method estimates canonical sampling probabilities by reweighting the obtained biased probabilities using the values of the boost potential at every point of the PMF. The variables used to build a bi-dimensional PMF were the x and y coordinates of the spermine's center of mass. Before the extraction of the variables' values, the simulation trajectories were processed using periodic boundary conditions in the way that the CXCR4 receptor is placed in the center of the plane xy, which corresponds to the membrane plane. Fifteen thousand trajectory frames (covering 300 ns of simulation) were extracted from the region of minimum free energy in the PMF, which contains the binding sites in the receptor. These frames were clustered using a quality threshold–based algorithm (*76*) implemented in VMD (*77*) with a root mean square deviation (RMSD) threshold of 5 Å between conformations of the spermine molecule (before the RMSD calculations, the receptor structure was aligned among all the frames to obtain a fixed reference to the position of the spermine). Three clusters were extracted from this analysis, which gather 43.3, 29.8, and 12.4% of the sampling, respectively.

The contacts between spermine and CXCR4 were defined by the heavy atoms of either molecule located at the cutoff distance of 4 Å. The contact frequency was calculated as the number of frames with contacts divided by the total frames of the production GaMD simulations.

Molecular docking was performed with LeDock (*78*). The starting structures of the ligands were obtained from the ZINC database (*79*): spermine (ZINC1532734), putrescine (ZINC5828633), and ornithine (ZINC5828633). For all simulations, a docking box was defined comprising the whole binding region of CXCR4, with dimensions of 38.17 Å by 29.82 Å by 56.36 Å. For each system, a maximum of 10,000 solutions were explored. Solutions among the top 10% best-scored (*80*) were analyzed with UCSF Chimera (*81*).

Statistical analysis

IC_{50} values were calculated by nonlinear regression. Statistics were performed using GraphPad Prism (version 9.3.1).

Supplementary Materials

This PDF file includes:
Figs. S1 to S15
Tables S1 and S2
Legends for data S1 to S3

Other Supplementary Material for this manuscript includes the following:
Data S1 to S3

View/request a protocol for this paper from *Bio-protocol*.

REFERENCES AND NOTES

1. S. G. Deeks, J. Overbaugh, A. Phillips, S. Buchbinder, HIV infection. *Nat. Rev. Dis. Primers* **1**, 15035 (2015).
2. E. Vicenzi, P. Lió, G. Poli, The puzzling role of CXCR4 in human immunodeficiency virus infection. *Theranostics* **3**, 18–25 (2013).
3. H. Schuitemaker, M. Koot, N. A. Kootstra, M. W. Dercksen, R. E. de Goede, R. P. van Steenwijk, J. M. Lange, J. K. Schattenkerk, F. Miedema, M. Tersmette, Biological phenotype of human immunodeficiency virus type 1 clones at different stages of infection: Progression of disease is associated with a shift from monocytotropic to T-cell-tropic virus population. *J. Virol.* **66**, 1354–1360 (1992).
4. B. Schramm, M. L. Penn, R. F. Speck, S. Y. Chan, E. De Clercq, D. Schols, R. I. Connor, M. A. Goldsmith, Viral entry through CXCR4 is a pathogenic factor and therapeutic target in human immunodeficiency virus type 1 disease. *J. Virol.* **74**, 184–192 (2000).
5. M. Koot, I. P. Keet, A. H. Vos, R. E. de Goede, M. T. Roos, R. A. Coutinho, F. Miedema, P. T. Schellekens, M. Tersmette, Prognostic value of HIV-1 syncytium-inducing phenotype for rate of $CD4^+$ cell depletion and progression to AIDS. *Ann. Intern. Med.* **118**, 681–688 (1993).
6. E. De Clercq, Mozobil® (Plerixafor, AMD3100), 10 years after its approval by the US Food and Drug Administration. *Antivir. Chem. Chemother.* **27**, 204020661982938 (2019).
7. J. S. Hunt, F. Romanelli, Maraviroc, a CCR5 coreceptor antagonist that blocks entry of human immunodeficiency virus type 1. *Pharmacotherapy* **29**, 295–304 (2009).
8. Word Health Organization, HIV/AIDS (2020); www.who.int/health-topics/hiv-aids/#tab=tab_1.
9. A. T. Haase, Targeting early infection to prevent HIV-1 mucosal transmission. *Nature* **464**, 217–223 (2010).
10. B. F. Keele, C. A. Derdeyn, Genetic and antigenic features of the transmitted virus. *Curr. Opin. HIV AIDS* **4**, 352–357 (2009).
11. R. E. Haaland, P. A. Hawkins, J. Salazar-Gonzalez, A. Johnson, A. Tichacek, E. Karita, O. Manigart, J. Mulenga, B. F. Keele, G. M. Shaw, B. H. Hahn, S. A. Allen, C. A. Derdeyn, E. Hunter, Inflammatory genital infections mitigate a severe genetic bottleneck in heterosexual transmission of subtype A and C HIV-1. *PLOS Pathog.* **5**, e1000274 (2009).
12. C. A. Derdeyn, Envelope-constrained neutralization-sensitive HIV-1 after heterosexual transmission. *Science* **303**, 2019–2022 (2004).
13. J. F. Salazar-Gonzalez, M. G. Salazar, B. F. Keele, G. H. Learn, E. E. Giorgi, H. Li, J. M. Decker, S. Wang, J. Baalwa, M. H. Kraus, N. F. Parrish, K. S. Shaw, M. B. Guffey, K. J. Bar, K. L. Davis, C. Ochsenbauer-Jambor, J. C. Kappes, M. S. Saag, M. S. Cohen, J. Mulenga, C. A. Derdeyn, S. Allen, E. Hunter, M. Markowitz, P. Hraber, A. S. Perelson, T. Bhattacharya, B. F. Haynes, B. T. Korber, B. H. Hahn, G. M. Shaw, Genetic identity, biological phenotype, and evolutionary pathways of transmitted/founder viruses in acute and early HIV-1 infection. *J. Exp. Med.* **206**, 1273–1289 (2009).
14. N. F. Parrish, F. Gao, H. Li, E. E. Giorgi, H. J. Barbian, E. H. Parrish, L. Zajic, S. S. Iyer, J. M. Decker, A. Kumar, B. Hora, A. Berg, F. Cai, J. Hopper, T. N. Denny, H. Ding, C. Ochsenbauer, J. C. Kappes, R. P. Galimidi, A. P. West, P. J. Bjorkman, C. B. Wilen, R. W. Doms, M. O'Brien, N. Bhardwaj, P. Borrow, B. F. Haynes, M. Muldoon, J. P. Theiler, B. Korber, G. M. Shaw, B. H. Hahn, Phenotypic properties of transmitted founder HIV-1. *Proc. Natl. Acad. Sci. U.S.A.* **110**, 6626–6633 (2013).
15. B. F. Keele, E. E. Giorgi, J. F. Salazar-Gonzalez, J. M. Decker, K. T. Pham, M. G. Salazar, C. Sun, T. Grayson, S. Wang, H. Li, X. Wei, C. Jiang, J. L. Kirchherr, F. Gao, J. A. Anderson, L.-H. Ping, R. Swanstrom, G. D. Tomaras, W. A. Blattner, P. A. Goepfert, J. M. Kilby, M. S. Saag, E. L. Delwart, M. P. Busch, M. S. Cohen, D. C. Montefiori, B. F. Haynes, B. Gaschen, G. S. Athreya, H. Y. Lee, N. Wood, C. Seoighe, A. S. Perelson, T. Bhattacharya, B. T. Korber, B. H. Hahn, G. M. Shaw, Identification and characterization of transmitted and early founder virus envelopes in primary HIV-1 infection. *Proc. Natl. Acad. Sci. U.S.A.* **105**, 7552–7557 (2008).
16. M.-R. Abrahams, J. A. Anderson, E. E. Giorgi, C. Seoighe, K. Mlisana, L.-H. Ping, G. S. Athreya, F. K. Treurnicht, B. F. Keele, N. Wood, J. F. Salazar-Gonzalez, T. Bhattacharya, H. Chu, I. Hoffman, S. Galvin, C. Mapanje, P. Kazembe, R. Thebus, S. Fiscus, W. Hide, M. S. Cohen, S. A. Karim, B. F. Haynes, G. M. Shaw, B. H. Hahn, B. T. Korber, R. Swanstrom, C. Williamson, Quantitating the multiplicity of infection with human immunodeficiency virus type 1 subtype C reveals a non-poisson distribution of transmitted variants. *J. Virol.* **83**, 3556–3567 (2009).
17. B. F. Keele, H. Li, G. H. Learn, P. Hraber, E. E. Giorgi, T. Grayson, C. Sun, Y. Chen, W. W. Yeh, N. L. Letvin, J. R. Mascola, G. J. Nabel, B. F. Haynes, T. Bhattacharya, A. S. Perelson, B. T. Korber, B. H. Hahn, G. M. Shaw, Low-dose rectal inoculation of rhesus macaques by SIVsmE660 or SIVmac251 recapitulates human mucosal infection by HIV-1. *J. Exp. Med.* **206**, 1117–1134 (2009).

18. K. Terahara, M. Ishige, S. Ikeno, S. Okada, M. Kobayashi-Ishihara, M. Ato, Y. Tsunetsugu-Yokota, Humanized mice dually challenged with R5 and X4 HIV-1 show preferential R5 viremia and restricted X4 infection of $CCR5^+CD4^+$ T cells. *Microbes Infect.* **17**, 378–386 (2015).
19. L. Margolis, R. Shattock, Selective transmission of CCR5-utilizing HIV-1: The "gatekeeper" problem resolved? *Nat. Rev. Microbiol.* **4**, 312–317 (2006).
20. J.-C. Grivel, R. J. Shattock, L. B. Margolis, Selective transmission of R5 HIV-1 variants: Where is the gatekeeper? *J. Transl. Med.* **9**, S6 (2010).
21. S. Yandrapally, K. Mohareer, G. Arekuti, G. R. Vadankula, S. Banerjee, HIV co-receptor-tropism: Cellular and molecular events behind the enigmatic co-receptor switching. *Crit. Rev. Microbiol.* **47**, 499–516 (2021).
22. S. B. Joseph, R. Swanstrom, A. D. M. Kashuba, M. S. Cohen, A. D. M. Kashuba, M. S. Cohen, Bottlenecks in HIV-1 transmission: Insights from the study of founder viruses. *Nat. Rev. Microbiol.* **13**, 414–425 (2015).
23. M. Cornelissen, G. Mulder-Kampinga, J. Veenstra, F. Zorgdrager, C. Kuiken, S. Hartman, J. Dekker, L. van der Hoek, C. Sol, R. Coutinho, Syncytium-inducing (SI) phenotype suppression at seroconversion after intramuscular inoculation of a non-syncytium-inducing/SI phenotypically mixed human immunodeficiency virus population. *J. Virol.* **69**, 1810–1818 (1995).
24. J. L. Lathey, R. D. Pratt, S. A. Spector, Appearance of autologous neutralizing antibody correlates with reduction in virus load and phenotype switch during primary infection with human immunodeficiency virus type 1. *J. Infect. Dis.* **175**, 231–232 (1997).
25. S. Fais, C. Lapenta, S. M. Santini, M. Spada, S. Parlato, M. Logozzi, P. Rizza, F. Belardelli, Human immunodeficiency virus type 1 strains R5 and X4 induce different pathogenic effects in hu-PBL-SCID mice, depending on the state of activation/differentiation of human target cells at the time of primary infection. *J. Virol.* **73**, 6453–6459 (1999).
26. J. M. Harouse, C. Buckner, A. Gettie, R. Fuller, R. Bohm, J. Blanchard, C. Cheng-Mayer, $CD8^+$ T cell-mediated CXC chemokine receptor 4-simian/human immunodeficiency virus suppression in dually infected rhesus macaques. *Proc. Natl. Acad. Sci. U.S.A.* **100**, 10977–10982 (2003).
27. G. R. Yeaman, S. Asin, S. Weldon, D. J. Demian, J. E. Collins, J. L. Gonzalez, C. R. Wira, M. W. Fanger, A. L. Howell, Chemokine receptor expression in the human ectocervix: Implications for infection by the human immunodeficiency virus-type I. *Immunology* **113**, 524–533 (2004).
28. E. Saba, J.-C. Grivel, C. Vanpouille, B. Brichacek, W. Fitzgerald, L. Margolis, A. Lisco, HIV-1 sexual transmission: Early events of HIV-1 infection of human cervico-vaginal tissue in an optimized ex vivo model. *Mucosal Immunol.* **3**, 280–290 (2010).
29. B. K. Patterson, A. Landay, J. Andersson, C. Brown, H. Behbahani, D. Jiyamapa, Z. Burki, D. Stanislawski, M. A. Czerniewski, P. Garcia, Repertoire of chemokine receptor expression in the female genital tract: Implications for human immunodeficiency virus transmission. *Am. J. Pathol.* **153**, 481–490 (1998).
30. S. G. McCoombe, R. V. Short, Potential HIV-1 target cells in the human penis. *AIDS* **20**, 1491–1495 (2006).
31. O. D. Council, M. D. Swanson, R. A. Spagnuolo, A. Wahl, J. V. Garcia, Role of semen on vaginal HIV-1 transmission and maraviroc protection. *Antimicrob. Agents Chemother.* **59**, 7847–7851 (2015).
32. J.-C. Grivel, J. Elliott, A. Lisco, A. Biancotto, C. Condack, R. J. Shattock, I. McGowan, L. Margolis, P. Anton, HIV-1 pathogenesis differs in rectosigmoid and tonsillar tissues infected ex vivo with CCR5- and CXCR4-tropic HIV-1. *AIDS* **21**, 1263–1272 (2007).
33. R. Sarrami-Forooshani, A. W. Mesman, N. H. van Teijlingen, J. K. Sprokholt, M. van der Vlist, C. M. S. Ribeiro, T. B. H. Geijtenbeek, Human immature Langerhans cells restrict CXCR4-using HIV-1 transmission. *Retrovirology* **11**, 52 (2014).
34. M. Prakash, M. S. Kapembwa, F. Gotch, S. Patterson, Chemokine receptor expression on mucosal dendritic cells from the endocervix of healthy women. *J. Infect. Dis.* **190**, 246–250 (2004).
35. L. Mayr, B. Su, C. Moog, Langerhans cells: The 'Yin and Yang' of HIV restriction and transmission. *Trends Microbiol.* **25**, 170–172 (2017).
36. N. Nasr, J. Lai, R. A. Botting, S. K. Mercier, A. N. Harman, M. Kim, S. Turville, R. J. Center, T. Domagala, P. R. Gorry, N. Olbourne, A. L. Cunningham, Inhibition of two temporal phases of HIV-1 transfer from primary langerhans cells to T cells: The role of langerin. *J. Immunol.* **193**, 2554–2564 (2014).
37. M. Cavarelli, C. Foglieni, M. Rescigno, G. Scarlatti, R5 HIV-1 envelope attracts dendritic cells to cross the human intestinal epithelium and sample luminal virions via engagement of the CCR5. *EMBO Mol. Med.* **5**, 776–794 (2013).
38. R. A. Botting, H. Rana, K. M. Bertram, J. W. Rhodes, H. Baharlou, N. Nasr, A. L. Cunningham, A. N. Harman, Langerhans cells and sexual transmission of HIV and HSV. *Rev. Med. Virol.* **27**, e1923 (2017).
39. B. Shohat, R. Maayan, R. Singer, M. Sagiv, H. Kaufman, Z. Zukerman, Immunosuppressive activity and polyamine levels of seminal plasma in azo-ospermic, oligospermic, and normospermic men. *Arch. Androl.* **24**, 41–50 (1990).
40. A. Papkalla, J. Münch, C. Otto, F. Kirchhoff, Nef enhances human immunodeficiency virus type 1 infectivity and replication independently of viral coreceptor tropism. *J. Virol.* **76**, 8455–8459 (2002).
41. M. Harms, P. von Maltitz, B. Mayer, M. Deniz, J. Müller, J. Münch, Utilization of amino-guanidine prevents cytotoxic effects of semen. *Int. J. Mol. Sci.* **23**, 8563 (2022).
42. C. E. Holbert, M. Dunworth, J. R. Foley, T. T. Dunston, T. M. Stewart, R. A. Casero, Autophagy induction by exogenous polyamines is an artifact of bovine serum amine oxidase activity in culture serum. *J. Biol. Chem.* **295**, 9061–9068 (2020).
43. M. Han, M. Woottum, R. Mascarau, Z. Vahlas, C. Verollet, S. Benichou, Mechanisms of HIV-1 cell-to-cell transfer to myeloid cells. *J. Leukoc. Biol.* **112**, 1261–1271 (2022).
44. L. Bracq, M. Xie, S. Benichou, J. Bouchet, Mechanisms for cell-to-cell transmission of HIV-1. *Front. Immunol.* **9**, 260 (2018).
45. M. Han, V. Cantaloube-Ferrieu, M. Xie, M. Armani-Tourret, M. Woottum, J.-C. Pagès, P. Colin, B. Lagane, S. Benichou, HIV-1 cell-to-cell spread overcomes the virus entry block of non-macrophage-tropic strains in macrophages. *PLOS Pathog.* **18**, e1010335 (2022).
46. L. Bracq, M. Xie, M. Lambelé, L.-T. Vu, J. Matz, A. Schmitt, J. Delon, P. Zhou, C. Randriamampita, J. Bouchet, S. Benichou, T cell-macrophage fusion triggers multinucleated giant cell formation for HIV-1 spreading. *J. Virol.* **91**, e01237-17 (2017).
47. B. Wu, E. Y. T. T. Chien, C. D. Mol, G. Fenalti, W. Liu, V. Katritch, R. Abagyan, A. Brooun, P. Wells, F. C. Bi, D. J. Hamel, P. Kuhn, T. M. Handel, V. Cherezov, R. C. Stevens, Structures of the CXCR4 chemokine GPCR with small-molecule and cyclic peptide antagonists. *Science* **330**, 1066–1071 (2010).
48. A. Boonen, A. K. Singh, A. Van Hout, K. Das, T. Van Loy, S. Noppen, D. Schols, Development of a novel SPR assay to study CXCR4-ligand interactions. *Biosensors* **10**, 150 (2020).
49. M. Harms, A. Gilg, L. Ständker, A. J. Beer, B. Mayer, V. Rasche, C. W. Gruber, J. Münch, Microtiter plate-based antibody-competition assay to determine binding affinities and plasma/blood stability of CXCR4 ligands. *Sci. Rep.* **10**, 16036 (2020).
50. P. J. Oefner, S. Wongyai, G. Bonn, High-performance liquid chromatographic determination of free polyamines in human seminal plasma. *Clin. Chim. Acta* **205**, 11–18 (1992).
51. H. Jakobsen, H. Rui, Y. Thomassen, T. Hald, K. Purvis, Polyamines and other accessory sex gland secretions in human seminal plasma 8 years after vasectomy. *Reproduction* **87**, 39–45 (1989).
52. J. Jänne, E. Hölttä, P. Haaranen, K. Elfving, Polyamines and polyamine-metabolizing enzyme activities in human semen. *Clin. Chim. Acta* **48**, 393–401 (1973).
53. R. D. Allen, T. K. Roberts, Role of spermine in the cytotoxic effects of seminal plasma. *Am. J. Reprod. Immunol. Microbiol.* **13**, 4–8 (1987).
54. K.-A. Kim, M. Yolamanova, O. Zirafi, N. R. Roan, L. Staendker, W.-G. Forssmann, A. Burgener, N. Dejucq-Rainsford, B. H. Hahn, G. M. Shaw, W. C. Greene, F. Kirchhoff, J. Münch, Semen-mediated enhancement of HIV infection is donor-dependent and correlates with the levels of SEVI. *Retrovirology* **7**, 55 (2010).
55. J. Münch, E. Rücker, L. Ständker, K. Adermann, C. Goffinet, M. Schindler, S. Wildum, R. Chinnadurai, D. Rajan, A. Specht, G. Giménez-Gallego, P. C. Sánchez, D. M. Fowler, A. Koulov, J. W. Kelly, W. Mothes, J.-C. C. Grivel, L. Margolis, O. T. Keppler, W.-G. G. Forssmann, F. Kirchhoff, Semen-derived amyloid fibrils drastically enhance HIV infection. *Cell* **131**, 1059–1071 (2007).
56. O. Zirafi, K.-A. A. Kim, N. R. Roan, S. F. Kluge, J. A. Müller, S. Jiang, B. Mayer, W. C. Greene, F. Kirchhoff, J. Münch, Semen enhances HIV infectivity and impairs the antiviral efficacy of microbicides. *Sci. Transl. Med.* **6**, 262ra157 (2014).
57. P. Tamamis, C. A. Floudas, Molecular recognition of CXCR4 by a dual tropic HIV-1 gp120 V3 loop. *Biophys. J.* **105**, 1502–1514 (2013).
58. P. L. C. Lefèvre, M.-F. Palin, B. D. Murphy, Polyamines on the reproductive landscape. *Endocr. Rev.* **32**, 694–712 (2011).
59. N. Smith, N. Pietrancosta, S. Davidson, J. Dutrieux, L. Chauveau, P. Cutolo, M. Dy, D. Scott-Algara, B. Manoury, O. Zirafi, I. McCort-Tranchepain, T. Durroux, F. Bachelerie, O. Schwartz, J. Münch, A. Wack, S. Nisole, J.-P. Herbeuval, Natural amines inhibit activation of human plasmacytoid dendritic cells through CXCR4 engagement. *Nat. Commun.* **8**, 14253 (2017).
60. N. Smith, M. P. M. P. Rodero, N. Bekaddour, V. Bondet, Y. B. Y. B. Ruiz-Blanco, M. Harms, B. Mayer, B. Bader-Meunier, P. Quartier, C. Bodemer, V. Baudouin, Y. Dieudonné, F. Kirchhoff, E. Sanchez Garcia, B. Charbit, N. Leboulanger, B. Jahrsdörfer, Y. Richard, A.-S. A.-S. Korganow, J. Münch, S. Nisole, D. Duffy, J.-P. J.-P. Herbeuval, Control of TLR7-mediated type I IFN signaling in pDCs through CXCR4 engagement—A new target for lupus treatment. *Sci. Adv.* **5**, eaav9019 (2019).
61. D. Kmiec, S. S. Iyer, C. M. Stürzel, D. Sauter, B. H. Hahn, F. Kirchhoff, Vpu-mediated counteraction of tetherin is a major determinant of HIV-1 interferon resistance. *MBio* **7**, e00934-16 (2016).

62. P. Sokkar, M. Harms, C. Stürzel, A. Gilg, G. Kizilsavas, M. Raasholm, N. Preising, M. Wagner, F. Kirchhoff, L. Ständker, G. Weidinger, B. Mayer, J. Münch, E. Sanchez-Garcia, Computational modeling and experimental validation of the EPI-X4/CXCR4 complex allows rational design of small peptide antagonists. *Commun. Biol.* **4**, 1113 (2021).
63. C. T. Veldkamp, C. Seibert, F. C. Peterson, N. B. De la Cruz, J. C. Haugner, H. Basnet, T. P. Sakmar, B. F. Volkman, Structural basis of CXCR4 sulfotyrosine recognition by the chemokine SDF-1/CXCL12. *Sci. Signal.* **1**, ra4 (2008).
64. W. L. Jorgensen, J. Chandrasekhar, J. D. Madura, R. W. Impey, M. L. Klein, Comparison of simple potential functions for simulating liquid water. *J. Chem. Phys.* **79**, 926–935 (1983).
65. S. Jo, T. Kim, V. G. Iyer, W. Im, CHARMM-GUI: A web-based graphical user interface for CHARMM. *J. Comput. Chem.* **29**, 1859–1865 (2008).
66. B. R. Brooks, C. L. Brooks, A. D. Mackerell, L. Nilsson, R. J. Petrella, B. Roux, Y. Won, G. Archontis, C. Bartels, S. Boresch, A. Caflisch, L. Caves, Q. Cui, A. R. Dinner, M. Feig, S. Fischer, J. Gao, M. Hodoscek, W. Im, K. Kuczera, T. Lazaridis, J. Ma, V. Ovchinnikov, E. Paci, R. W. Pastor, C. B. Post, J. Z. Pu, M. Schaefer, B. Tidor, R. M. Venable, H. L. Woodcock, X. Wu, W. Yang, D. M. York, M. Karplus, CHARMM: The biomolecular simulation program. *J. Comput. Chem.* **30**, 1545–1614 (2009).
67. J. Lee, X. Cheng, J. M. Swails, M. S. Yeom, P. K. Eastman, J. A. Lemkul, S. Wei, J. Buckner, J. C. Jeong, Y. Qi, S. Jo, V. S. Pande, D. A. Case, C. L. Brooks, A. D. MacKerell, J. B. Klauda, W. Im, CHARMM-GUI input generator for NAMD, GROMACS, AMBER, OpenMM, and CHARMM/OpenMM simulations using the CHARMM36 additive force field. *J. Chem. Theory Comput.* **12**, 405–413 (2016).
68. Y. T. Pang, Y. Miao, Y. Wang, J. A. McCammon, Gaussian accelerated molecular dynamics in NAMD. *J. Chem. Theory Comput.* **13**, 9–19 (2017).
69. T. Darden, D. York, L. Pedersen, Particle mesh Ewald: An N·log(N) method for Ewald sums in large systems. *J. Chem. Phys.* **98**, 10089–10092 (1993).
70. G. J. Martyna, D. J. Tobias, M. L. Klein, Constant pressure molecular dynamics algorithms. *J. Chem. Phys.* **101**, 4177–4189 (1994).
71. S. E. Feller, Y. Zhang, R. W. Pastor, B. R. Brooks, Constant pressure molecular dynamics simulation: The Langevin piston method. *J. Chem. Phys.* **103**, 4613–4621 (1995).
72. J. Huang, A. D. MacKerell, CHARMM36 all-atom additive protein force field: Validation based on comparison to NMR data. *J. Comput. Chem.* **34**, 2135–2145 (2013).
73. J. C. Phillips, R. Braun, W. Wang, J. Gumbart, E. Tajkhorshid, E. Villa, C. Chipot, R. D. Skeel, L. Kalé, K. Schulten, Scalable molecular dynamics with NAMD. *J. Comput. Chem.* **26**, 1781–1802 (2005).
74. J. G. Kirkwood, Statistical mechanics of fluid mixtures. *J. Chem. Phys.* **3**, 300–313 (1935).
75. Y. Miao, W. Sinko, L. Pierce, D. Bucher, R. C. Walker, J. A. McCammon, Improved reweighting of accelerated molecular dynamics simulations for free energy calculation. *J. Chem. Theory Comput.* **10**, 2677–2689 (2014).
76. L. J. Heyer, S. Kruglyak, S. Yooseph, Exploring expression data: Identification and analysis of coexpressed genes. *Genome Res.* **9**, 1106–1115 (1999).
77. W. Humphrey, A. Dalke, K. Schulten, VMD: Visual molecular dynamics. *J. Mol. Graph.* **14**, 27–28 (1996).
78. H. Zhao, A. Caflisch, Discovery of ZAP70 inhibitors by high-throughput docking into a conformation of its kinase domain generated by molecular dynamics. *Bioorg. Med. Chem. Lett.* **23**, 5721–5726 (2013).
79. J. J. Irwin, K. G. Tang, J. Young, C. Dandarchuluun, B. R. Wong, M. Khurelbaatar, Y. S. Moroz, J. Mayfield, R. A. Sayle, ZINC20-a free ultralarge-scale chemical database for ligand discovery. *J. Chem. Inf. Model.* **60**, 6065–6073 (2020).
80. B. J. Bender, S. Gahbauer, A. Luttens, J. Lyu, C. M. Webb, R. M. Stein, E. A. Fink, T. E. Balius, J. Carlsson, J. J. Irwin, B. K. Shoichet, A practical guide to large-scale docking. *Nat. Protoc.* **16**, 4799–4832 (2021).
81. E. F. Pettersen, T. D. Goddard, C. C. Huang, G. S. Couch, D. M. Greenblatt, E. C. Meng, T. E. Ferrin, UCSF Chimera—A visualization system for exploratory research and analysis. *J. Comput. Chem.* **25**, 1605–1612 (2004).

Acknowledgments: We are grateful to all semen donors. Acetylated spermine was provided by R. Alves de Sousa (CNRS, Paris Descartes University). **Funding:** This work was supported by Deutsche Forschungsgemeinschaft CRC1279 (to J.M., Fl.K., and E.S.-G.); Deutsche Forschungsgemeinschaft MU3115 8-1 (to J.M.); Deutsche Forschungsgemeinschaft MU3115 11-1 (to J.M.); Deutsche Forschungsgemeinschaft SM544/1-1 (to N.S.); Deutsche Forschungsgemeinschaft 436586093 (to E.S.-G.); Baden-Württemberg Stiftung, Eliteprogramm für Postdocs (to M. Harms); Agence Nationale de Recherche sur le SIDA et les Hépatites Virales ANRS (to J.-P.H. and S.B.); China Scholarship Council CSC (to M. Han); EMBO long-term fellowship LT-834-2017 (to N.S.); SIDACTION 13151 (to N.S.); DFG under Germany's Excellence Strategy—EXC 2033—390677874—RESOLV (to E.S.-G.); Intramural funding of Ulm University —Equal Opportunities Unit (to M. Harms); Intramural funding of Ulm University —Bausteinprogramm—L.SBN.0209 (to M. Harms); Horizon Europe Framework Program; Marie Skłodowska-Curie Actions #101063953 Postdoctoral Fellowships 2021 (to B.C.); and Agence nationale de la Recherche ANR-21-CE15-0048 (to J.-P.H.) **Author contributions:** Conceptualization: M. Harms, N.S., E.S.-G., J.M., and J.-P.H. Methodology: M. Harms, C.S., N.S., R.G., A.R.-A., L.S., B.L., S.W., A.B., Y.B.R.-B., Y.A.-H., and B.T. Investigation: M. Harms, N.S., R.G., P.v.M., M. Han, S.S., N.B., D.C., and B.C. Confirmation: K.V. and Fr.K. Formal analysis: Y.B.R.-B., Y.A.-H., and E.S.-G. Visualization: M. Harms and N.S. Supervision: Fl.K., J.M., J.-P.H., S.B., D.S., and E.S.-G. Writing—original draft: M. Harms, N.S., Y.B.R.-B., E.S.-G., J.M., and J.-P.H. Writing—review and editing: E.S.-G., S.B., and J.M. **Competing interests:** The authors declare that they have no competing interests. **Data and materials availability:** All data needed to evaluate the conclusions in the paper are present in the paper and/or the Supplementary Materials. Primary data and computational data that support the findings of this study are available at https://data.mendeley.com/datasets/mznhj765w5/draft?a=c36862a3-547b-4d38-bdb3-98804a09a1ec (DOI:10.17632/mznhj765w5.1).

Submitted 15 November 2022
Accepted 1 June 2023
Published 5 July 2023
10.1126/sciadv.adf8251

ScienceAdvances

Spermine and spermidine bind CXCR4 and inhibit CXCR4- but not CCR5-tropic HIV-1 infection

Mirja Harms, Nikaïa Smith, Mingyu Han, Rüdiger Groß, Pascal von Maltitz, Christina Stürzel, Yasser B. Ruiz-Blanco, Yasser Almeida-Hernández, Armando Rodriguez-Alfonso, Dominique Cathelin, Birgit Caspar, Bouceba Tahar, Sophie Sayettat, Nassima Bekaddour, Kanika Vanshylla, Franziska Kleipass, Sebastian Wiese, Ludger Ständker, Florian Klein, Bernard Lagane, Arnaud Boonen, Dominique Schols, Serge Benichou, Elsa Sanchez-Garcia, Jean-Philippe Herbeuval, and Jan Münch

Sci. Adv. **9** (27), eadf8251. DOI: 10.1126/sciadv.adf8251